

Article

# Upgrading of Corn Stalk Residue and Tannery Waste into Sustainable Solid Biofuel via Conventional Hydrothermal Carbonization and Co-Hydrothermal Carbonization

Napat Kaewtrakulchai <sup>1,\*</sup>, Sirayu Chanpee <sup>2</sup>, Kanit Manatura <sup>3</sup>,  
Apiluck Eiad-Ua <sup>4</sup>

<sup>1</sup> Kasetsart Agricultural and Agro-Industrial Product Improvement Institute, Kasetsart University, Bangkok 10900, Thailand

<sup>2</sup> Department of Chemical Engineering, School of Engineering, King Mongkut's Institute of Technology, Bangkok 10520, Thailand

<sup>3</sup> Department of Mechanical Engineering, Faculty of Engineering at Kamphaeng Saen, Kasetsart University Kamphaeng Saen campus, Nakhon Pathom 73140, Thailand

<sup>4</sup> College of Material Innovation and Technology, King Mongkut's Institute of Technology, Bangkok 10520, Thailand

\* Correspondence: Napat Kaewtrakulchai, Email: knapat.kara@gmail.com.

---

## ABSTRACT

Hydrothermal carbonization (HTC) and co-hydrothermal carbonization (Co-HTC) are efficient thermochemical conversion processes for upgrading the fuel properties of biomass feedstocks. This study investigates the conversion of high moisture industrial waste, leather waste (LW), and agricultural residue, corn stalk (CS) into sustainable solid fuel via the HTC and Co-HTC. The impact of experimental variables, such as HTC temperature, residence time, and reaction pathway (i.e., HTC and Co-HTC process), on the physicochemical properties and fuel quality of hydrochar was also comprehensively explored. The highest heating value of hydrochar product, approximately 23.4 MJ/kg, was obtained from the Co-HTC condition of 280 °C for 8 h. The mutual interaction between two biowastes exhibited superior synergistic fuel characteristics, including lower ash content, higher carbon percentage, and improved energy density. However, the remaining ash content of hydrochar decreased by approximately 25.01%–44.52%, produced from both HTC and Co-HTC processes. The hydrothermal treatment process improved the hygroscopic properties of hydrochar. Finding results show that the HTC and Co-HTC are the potential thermochemical conversions for producing sustainable solid fuel from several biowastes. In addition, the Co-HTC process showed a better hydrochar fuel quality.

**KEYWORDS:** corn stalk; leather waste; hydrothermal carbonization; co-hydrothermal carbonization; solid biofuel

---

## Open Access

Received: 28 July 2023

Accepted: 13 October 2023

Published: 23 October 2023

Copyright © 2023 by the author(s). Licensee Hapres, London, United Kingdom. This is an open access article distributed under the terms and conditions of [Creative Commons Attribution 4.0 International License](https://creativecommons.org/licenses/by/4.0/).

## INTRODUCTION

Currently, energy consumption demand has sharply increased due to the skyrocketed growth of the population and industrialization [1]. Thus, the conversion of biowastes into a sustainable and clean energy source is a primary key challenge for decarbonization in industrial processing and electricity generation for solving environmental issues since the high consumption of petroleum fuel directly produces a severe problem regarding a large number of greenhouse gases (GHGs), particularly carbon dioxide (CO<sub>2</sub>) emission, and particulate matters. As an increase in the sustainable development concept, a large amount of unrecyclable waste has been refined into various forms of biofuels, such as solid biofuel, bio-oil, and combustible gas, instead of dropping into landfills [2,3]. Using waste biomass to obtain renewable energy becomes a practical pathway to net zero greenhouse gas emissions [4]. To date, several agricultural waste biomass and industrial wastes are widely supplied as potential feedstock for renewable energy production [3,5,6].

However, the utilization of raw biomass as solid fuel has experienced some severe problems due to the nature of raw biomass, which consists of high ash content and a variety of elemental compositions of ash contained during the biomass growth that causes slagging, fouling, agglomeration, and corrosion to combustion system [7]. According to literature reviews, silicon, potassium, calcium, and magnesium significantly cause depositions in the combustion system, reducing heat transfer efficiency. Chlorine, sulfur, and heavy metals can transform into hazardous air pollutants. However, the low heating value of raw biomass still needs to be improved to the high thermal efficient applications. The mentioned problems can be efficiently mitigated by biomass pretreatment, enhancing fuel properties [8,9].

In the biomass pretreatment process to decrease ash constituents, existing physical and chemical preprocessing techniques, including water washing at ambient temperature to near boiling and dilute acid/alkaline washing, are efficient for removing ash components [10]. Inorganic compositions contained in biomass feedstocks can decrease by washing method owing to the excellent water-solubility of metal ions in ash [11]. Even the silicon, calcium, and magnesium, which have low water solubility, can be significantly removed by the water leaching technique [12]. Nonetheless, the performance of ash washing generally depends on the operating conditions, such as particle size, biomass feedstock, temperature washing time, and water ratio. Increasing water temperature, water-to-biomass ratio, and washing time enhance the reduction of final ash content [7,13]. However, the present alkali in the washing method drastically increased the solubility of some elements such as SiO<sub>2</sub>, Al<sub>2</sub>O<sub>3</sub>, and MgO, typically significant ash in agricultural waste biomass [11,14–16]. Deng et al. (2013) reported the investigation of water washing on fuel properties of plant biomass and ash reduction efficiency at different washing temperatures and washing times. The fuel properties of raw

biomass are improved by water washing. Increasing the washing temperature is adequate for silicon removal [7]. A similar finding is consistent with the report of Bandara et al. (2020) that 88%–95% of potassium, 60%–83% of phosphorus, 38%–54% of iron, and 19%–24% of silicon contained in rice husk have been removed by water washing.

In recent years, numerous solid wastes have been used as raw materials for solid biofuel production via different thermal conversion techniques, such as torrefaction, carbonization, conventional hydrothermal carbonization (HTC), and co-hydrothermal carbonization (Co-HTC), to improve the heating value of biomass-derived solid fuel. The biomass-based solid fuel is effectively supplied for the combustion chamber and water boiler, substituted for fossil fuel consumption, corresponding to the decarbonization concept. Hydrothermal carbonization (HTC) is applied as a wet treatment process for highly moist biomass to produce solid biofuel derived from waste biomass [17]. The HTC process is typically conducted at a temperature between 180 and 300 °C for minutes to several hours using water as a reaction medium. The fuel qualities, including energy density, grind ability, and hygroscopic behavior, are enhanced using the hydrothermal carbonization (HTC) process. Several biomass feedstocks, such as olive stone [18], algae [19], rice husk [20], corn stalk [21], leather waste [22], and oily sludge [23], have been thoroughly evaluated by the HTC process for solid biofuel application.

Over the past few years, many researchers have worked on the co-hydrothermal carbonization (Co-HTC) of blended biomass feedstocks, and this process reveals some synergistic fuel properties of hydrochar products, such as superior chemical structure, mechanical strength, and uniformity [24–26]. Saba et al. (2017) studied the co-hydrothermal carbonization between coal and miscanthus. The hydrochar obtained from Co-HTC exhibited the shared fuel properties of low ash and sulfur content of miscanthus with high heating value maintaining of coal [27]. Kahilu et al. (2022) examined the physicochemical properties of Co-HTC hydrochar between coal slurry and sewage sludge. They revealed that the Co-HTC hydrochar yield was higher than the yield obtained from conventional HTC. In contrast, sulfur and ash content reduction was obtained for blending hydrochar, improving calorific value [28]. In addition, few published studies on Co-HTC between plant biomass and plastic wastes, particularly polyvinyl chloride (PVC), could be found over the last decade [26,29–31].

Nonetheless, the HTC and Co-HTC process may benefit the removal of ash constituents and increase calorific value simultaneously. The biomass structure is chemically reorganized by hydrolysis, dehydration, decarboxylation, aromatization, and recondensation, resulting in the formation of rich-carbon and high energy-dense products, often termed hydrochar. The inorganic molecules in the biomass structure may be removed in a liquid phase during the HTC process [32,33]. Zhang et al.

(2018) showed the improvement of bamboo sawdust's fuel properties obtained from several hydrothermal carbonization conditions. The elemental compositions, including K, Na, Mg, Ca, and S, were efficiently removed by the HTC process [34]. Also, a similar finding by Lin et al. (2019) showed that the HTC process has demonstrated the ability to remove the ash content contained in biomass. The HTC temperature and treatment time significantly affect the total ash content of biochar [35]. Also, Song et al. (2019) investigated the Co-HTC of sewage sludge and lignite. Results revealed that hydrochar from the Co-HTC process exhibited superior synergistic effects such as higher heating value, more fixed carbon content, and enhancement of O/C and H/C ratio that were affected by a mutual reaction between two different feedstocks during the Co-HTC process [36]. Mazumder et al. (2022) studied the Co-HTC between coal and food waste. Their finding showed decreased total ash, sulfur, and chloride content by blending food waste in the Co-HTC process [37].

To our knowledge, fewer studies previously investigated the Co-HTC of agricultural residue-industrial waste blend feedstocks. Therefore, this study aimed to investigate the influences of HTC and Co-HTC processes for converting corn stalk and leather waste into hydrochar as a sustainable solid fuel. Herein, types of biomass feedstocks (corn stalk and leather waste), reaction pathways (HTC and Co-HTC), and experimental variables (Temperature and residence time) are crucial factors for this study. The physicochemical properties and fuel characteristics of HTC/co-hydrochar products were studied using proximate and ultimate analysis, Field emission scanning electron microscope (FE-SEM), N<sub>2</sub> sorption analyzer, and bomb calorimeter. In addition, the equilibrium moisture content and water contact angle explain the water adsorption behavior. Furthermore, the resulting co-hydrochar was comprehensively examined on the fuel quality to explain the synergistic effects, such as chemical contents, total ash content, production yield, energy yield, calorific value, and hygroscopic property compared to conventional hydrochar. Nonetheless, this study supposes hydrothermal treatment has become a viable pathway for novel solid biofuel production from industrial biowaste and agricultural biomass.

## **MATERIALS AND METHODS**

### **Materials**

Corn stalk residue was collected from a local corn mill in Nakhon Ratchasima, Thailand, and leather waste was obtained from CPL Group Co., LTD in Samutprakarn, Thailand. The two feedstocks were severally rinsed with deionized water to remove contaminants. Then, the washed samples were left to air dry using an electrical hot-air oven (model Biobase BOV-V125F, China) at 105 °C for 24 h. The samples were mechanically crushed and subsequently sieved into a size between 30 and 50 mesh using

a milling machine and sieve shaker, respectively. Table 1 depicts the proximate and ultimate analysis of raw biomass feedstocks. Deionized water was produced from the Elix system using a Milli-Q Progard TS2 pretreatment pack.

**Table 1.** Proximate and ultimate analysis of corn stalk (CS), leather waste (LW), and blended feedstock (CSLW).

Property	CS	LW	CSLW
<b>Proximate analysis (weight (%), d.b.)</b>			
Volatile matters	78.5	84.2	82.1
Fixed carbon*	12.8	9.7	11.5
Ash	8.7	6.1	6.4
<b>Ultimate analysis (weight (%), d.a.f.)</b>			
C	41.24 ± 1.49	39.11 ± 1.06	39.25 ± 0.93
H	4.93 ± 0.25	7.24 ± 0.31	6.11 ± 0.52
N	0.91 ± 0.13	13.17 ± 0.86	6.93 ± 0.97
O*	52.64 ± 0.54	40.19 ± 0.95	47.43 ± 0.68
S	0.28 ± 0.07	0.32 ± 0.05	0.28 ± 0.08
Cl**	0.6	1.3	0.7
HHV (MJ/kg)	15.2 ± 1.33	11.2 ± 0.97	12.9 ± 0.28

Note: d.b.—dry basis, d.a.f. —dry-ash-free basis, \*calculated by difference, (means ± SD;  $n = 3$ ), \*\*separately analyzed by multi EA4000.

### Conventional HTC and Co-HTC Experiments

About 30 g of feedstock was mixed with deionized water with a feedstock/ water ratio of 1:10 by weight. All conventional HTC and Co-HTC experiments were carried out in a 500 mL custom-made stainless-steel hydrothermal system controlled with a proportional-integral-derivative (PID) controller, as displayed in the schematic diagram of Figure 1. Before the experiments, the sample autoclave was purged with nitrogen for 5 min to avoid the air inside the reactor system. The blended feedstock (CS and LW) with a constant weight ratio of 1:1 (CS-to-LW, w/w) was used for the Co-HTC process. All hydrothermal experiments were carried out at the different hydrothermal temperatures of 200, 240, and 280 °C and hydrothermal treatment times of 1, 4, and 8 h using a heating rate of 7 °C/min. After hydrothermal treatment, the sample autoclave was quenched to the ambient temperature by cold water flowing to suppress all reactions. Afterward, the solid product, hydrochar, was filtrated by vacuum using a separatory Büchner funnel (Jipo, Germany) with paper filters. Then, the hydrochar sample was dried at 105 °C in an oven overnight, ground into homogenized powder, and stored in a sealed bag for further characteristics analysis. Herein, the hydrochar samples are namely by name-temperature-time. Moreover, the hydrochar yield (HY) is

expressed by following Equation (1) based on a dry basis. HTC and Co-HTC performances were studied based on energy yield and enhancement ratio as follows Equations (2), and (3), respectively.

$$\text{Hydrochar yield (HY, \%)} = \frac{\text{Mass}_{\text{hydrochar}}}{\text{Mass}_{\text{raw biomass}}} \times 100 \quad (1)$$

$$\text{Enhancement ratio (ER, -)} = \frac{\text{HHV}_{\text{hydrochar}}}{\text{HHV}_{\text{raw biomass}}} \quad (2)$$

$$\text{Energy yield (EY, \%)} = \text{HY} \times \text{ER} \quad (3)$$

Moreover, the fuel ratio of hydrochar was determined using the Equation (4) below.

$$\text{Fuel ratio} = \frac{\text{Fixed carbon}}{\text{Volatile matters}} \quad (4)$$

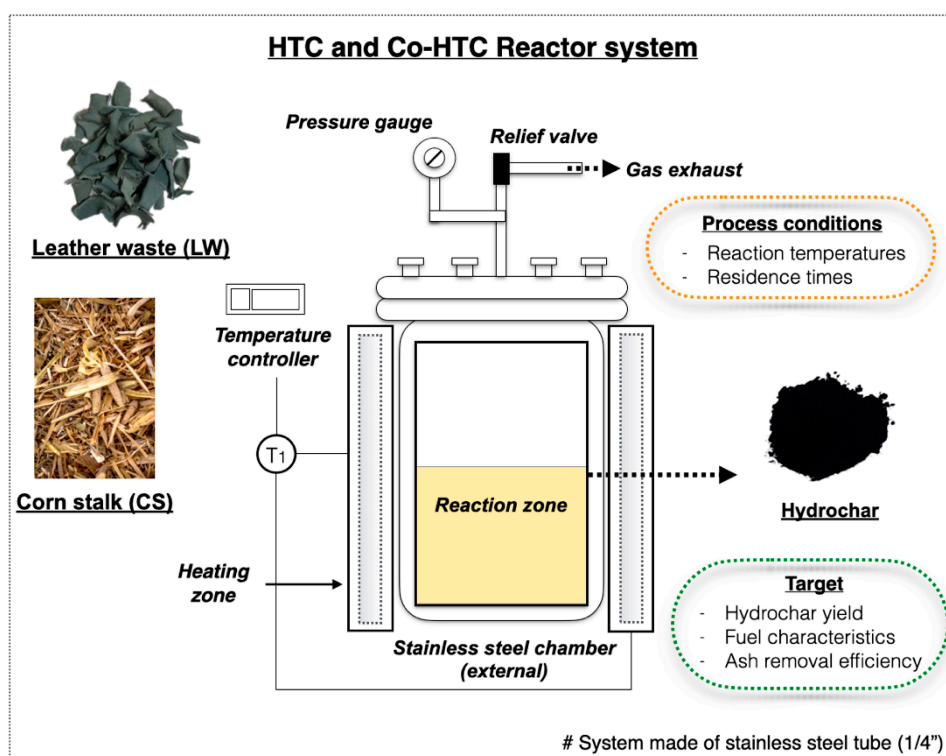


**Figure 1.** Schematic diagram of the hydrothermal reactor.

### Hydrochar Characterizations

The thermogravimetric analyzer (NETZSCH TG209, Germany) evaluates the proximate analysis of the raw feedstocks and hydrochar samples following the American Standard Test Method ASTM D 7582-15 (2015) for determining moisture, volatile matters, ash contents, and fixed carbon content by subtraction of others from 100%. The ultimate analysis was analyzed to determine the percentage of elemental composition, including carbon, hydrogen, nitrogen, oxygen, and sulfur, using a CHNS elemental analyzer modeled LECO Truspec CHN 628 (Netherlands)

following the ASTM D 5373-16 (2016) and ASTM D 4239-17 (2017), respectively. The chlorine (Cl) concentration was quantified using an elemental analyzer (multi EA4000, Analytik Jena, USA). A field emission scanning electron microscope (FE-SEM, Hitachi SU8030, Japan) displayed the surface morphology of hydrochar samples by using magnifications of 1000× magnification operated at a voltage of 5 kV. In addition, the porosity and specific surface area of hydrochars were determined to understand the transformation of surface morphology using an isothermal condition at -196 °C on a Quantachrome Autosorp IQ-MP-XR (Austria). The surface chemistry of raw feedstocks and hydrochar samples were studied by Fourier Transform Infrared Spectroscopy using FTIR PerkinElmer UATR Two (USA) in the wavenumber region of 4000–400 cm<sup>-1</sup> by direct impression technique for analysis. Calorific analysis of raw feedstock and hydrochar was analyzed by bomb calorimeter (IKA C5000, Germany) using the ASTM D 5865-13 (2013).

The equilibrium moisture content (EMC) percentage following Equation (4) explained the hygroscopic property. However, EMC testing was reached by storing dried samples in a desiccator with controlled 55% relative humidity at 30 °C for 24 h.  $Mass_{dried}$  and  $Mass_{wet}$  referred to the mass of dried and humidified samples, respectively. Meanwhile, the hygroscopicity reduction extent (HRE) was defined in Equation (5) to imply the reduction of feedstock hygroscopicity after the HTC/Co-HTC process. Moreover, the water contact angle on the sample surface demonstrates the hydrophobicity using an optical contact angle camera with a video measurement system.

$$\text{Equilibrium moisture content (EMC, \%)} = \frac{Mass_{wet} - Mass_{dried}}{Mass_{dried}} \times 100 \quad (5)$$

$$\text{Hygroscopicity reduction extent (HRE, \%)} = \left(1 - \frac{EMC_{hydrochar}}{EMC_{raw\ biomass}}\right) \times 100 \quad (6)$$

## RESULTS AND DISCUSSION

### Fuel Characteristics of HTC and Co-HTC Hydrochars

Initially, the CS and LW feedstocks were conducted through conventional hydrothermal carbonization at 200–280 °C for 1, 4, and 8 h to explore hydrothermal carbonization's effect on the fuel properties of hydrochar products. Table 2 reported the proximate and ultimate analyses. As seen in the finding results, the chemical contents (i.e., volatile matters, fixed carbon, and ash content) and elemental compositions, including C, H, N, O, and S, were significantly changed by the HTC. It can imply that the fuel property of raw feedstock significantly improved after the hydrothermal treatment. However, increasing the HTC temperature from 200 °C to 280 °C enhanced the devolatilization and carbonization

reactions, indicating that the thermal decomposition of oxygenated compounds and intra-C bonding occurred simultaneously [18]. This finding significantly resulted in a lowering of the volatile content of the hydrochar. They decreased from 78.5% to 51.8% for the CS sample and 84.2% to 54.7% for the LW sample, respectively. In addition, the highest FC content increase was approximately 41.4% for CS-280-8 and 38.6% for LW-280-8, respectively. Furthermore, increased HTC treatment time significantly affects the proximate and ultimate analyses of different hydrochar samples. The reaction time of the HTC process has the function of removing volatile matter and ash constituents [8,38].

**Table 2.** Fuel characteristics of HTC and Co-HTC products.

Samples	Conditions		Proximate analysis (% d.b.)		Ultimate analysis (% d.a.f.)					HHV (MJ/kg)	Fuel ratio
	T (°C)	t (h)	VM	FC*	A	C	H	N	O*		
Corn stalk (CS)	200	1	76.4	17.5	6.1	43.22 ± 1.09	4.21 ± 0.11	0.71 ± 0.07	51.86 ± 0.92	16.8 ± 0.8	0.22
		4	73.6	20.6	5.8	47.27 ± 0.95	3.63 ± 0.23	0.54 ± 0.09	48.56 ± 0.74	17.3 ± 0.8	0.27
		8	71.5	23.1	5.4	50.05 ± 0.99	3.24 ± 0.09	0.46 ± 0.11	46.25 ± 0.85	18.2 ± 0.4	0.32
	240	1	65.9	28.5	5.6	48.91 ± 1.02	4.07 ± 0.12	0.68 ± 0.13	46.34 ± 0.72	16.9 ± 0.5	0.43
		4	60.1	34.6	5.3	50.57 ± 0.96	3.59 ± 0.17	0.43 ± 0.09	45.41 ± 0.46	19.5 ± 0.5	0.57
		8	58.2	36.4	5.4	53.72 ± 0.58	3.45 ± 0.24	0.37 ± 0.08	42.46 ± 0.87	21.4 ± 0.4	0.62
	280	1	58.3	34.2	7.5	51.85 ± 0.79	4.22 ± 0.18	0.69 ± 0.09	43.24 ± 0.95	17.6 ± 0.3	0.58
		4	54.4	39.2	6.4	55.27 ± 1.01	3.76 ± 0.12	0.58 ± 0.10	40.39 ± 0.69	21.4 ± 0.2	0.72
		8	53.8	39.4	6.8	59.13 ± 0.79	3.54 ± 0.15	0.36 ± 0.16	36.97 ± 0.82	22.1 ± 0.1	0.73
Leather waste (LW)	200	1	79.6	14.5	5.9	46.81 ± 1.21	5.13 ± 0.12	7.32 ± 0.13	40.74 ± 0.94	16.7 ± 0.2	0.18
		4	77.1	17.8	5.1	50.67 ± 0.95	4.46 ± 0.34	5.41 ± 0.22	39.46 ± 1.02	18.5 ± 0.4	0.22
		8	75.3	18.4	6.3	51.23 ± 1.35	3.12 ± 0.11	4.25 ± 0.64	41.40 ± 0.83	21.6 ± 0.3	0.24
	240	1	78.2	16.6	5.2	51.31 ± 1.04	3.95 ± 0.25	5.31 ± 0.47	39.43 ± 1.15	19.9 ± 0.1	0.21
		4	66.5	28.1	5.4	53.77 ± 1.09	3.31 ± 0.53	4.95 ± 0.85	37.97 ± 0.86	19.7 ± 0.5	0.42
		8	62.1	32.0	5.9	56.19 ± 0.86	3.44 ± 0.37	3.86 ± 0.39	36.51 ± 0.99	22.3 ± 0.2	0.51
	280	1	76.8	16.7	6.5	52.54 ± 1.12	3.97 ± 0.51	6.42 ± 0.25	37.07 ± 0.93	20.6 ± 0.2	0.21
		4	56.8	37.3	5.9	56.45 ± 0.98	3.42 ± 0.21	4.51 ± 0.51	35.62 ± 1.07	21.7 ± 0.3	0.65
		8	54.7	38.6	6.7	57.91 ± 1.05	3.68 ± 0.16	4.89 ± 0.62	33.52 ± 1.01	22.5 ± 0.1	0.70
blend CSLW	200		75.9	19.7	4.4	49.31 ± 0.72	3.85 ± 0.23	2.76 ± 0.18	44.08 ± 1.13	18.1 ± 0.2	0.25
	240	4	56.1	38.8	5.1	53.89 ± 0.88	3.36 ± 0.19	2.27 ± 0.11	40.48 ± 0.99	22.9 ± 0.1	0.69
	280		53.7	40.9	5.4	55.31 ± 0.91	3.14 ± 0.42	2.42 ± 0.09	39.13 ± 1.05	23.4 ± 0.2	0.76

Note: d.b. —dry basis, d.a.f. —dry-ash-free basis, \*calculated by difference, (means ± SD; n = 3), VM—Volatile matter, FC—Fixed carbon, A—Ash.

Regarding ash reduction capacity during the HTC process, the inorganic molecules maintained in the ash can be decreased during the HTC reaction because the water medium of HTC could dissolve those of ash constituents. However, the removal efficiency significantly depends on the HTC parameters, and its elemental compositions led to different solubility [14,35,39]. On the contrary, the findings revealed that the decrease in total ash content is obtained from the initial stage to 4 h interval time. Nonetheless, the ash yield of HTC samples significantly returned when the HTC reaction time was increased from 4 h to 8 h, indicating that the re-

polymerization of dissolved ash composition occurred over a long period of the HTC process. This phenomenon also correlated with the increase in hydrochar yield when HTC reaction time increased from 4 h to 8 h. According to proximate analyses, an increase in the FC content as well as a decrease in VM content results in the enhancement of heating value, with the highest being 23.3 MJ/kg for CS hydrochar and 25.5 MJ/kg for LW hydrochar, which are close to those of natural coals such as lignite, sub-bituminous and bituminous coal. The fuel ratios of different hydrochars were relatively dependent on the HTC parameters. The highest fuel ratio was 0.79 and 0.70 for CS-280-8 and LW-280-8, respectively. The improving fuel ratio suggests that more FC content was obtained for hydrochar products favorable for their combustion behavior [40,41]. In addition, the ultimate analysis revealed that the carbon percentage increased, but the oxygen percentage continuously decreased concerning the HTC temperature and time. The carbon percentage was between 43.22%–59.13% for CS hydrochars and 46.81%–57.91% for LW hydrochars, respectively (see Table 2). The elemental hydrogen percentage decreased due to the dehydration reaction during the HTC process. Nitrogen content was relatively high for LW hydrochars, concerning the nature of raw leather waste [22,42].

According to the proximate analyses, the HTC reaction time of 4 h was selected for the Co-HTC process using different hydrothermal temperatures because the long hydrothermal reaction period can significantly enhance the re-polymerization of ash. Results showed that the carbon percentage increased, and the amount of ash constituent also raised after 4 h interval time, as demonstrated in Table 2. The high ash content is not favorable for any combustion process. The increase in ash content may suggest the lowering of hydrochar energy content. However, the high ash content in untreated feedstocks significantly decreased after the HTC or Co-HTC process by transforming the inorganic elements in the liquid phase [43]. The hydrothermal temperature significantly affects the fuel property. The fixed carbon content of Co-HTC products has increased about 3.17 times at Co-HTC of 280 °C from raw blended feedstock. The volatile matter and ash contents gradually decreased due to the thermal decomposition in a hot-compress water-surrounding environment, and the oxygenated compounds and inorganic elements were released simultaneously from the solid sample into the liquid and gas phase. This results in the direct reduction of hydrochar/co-hydrochar production yield. The volatile matter and ash contents of co-hydrochar were 53.7%–75.9%, and 4.4%–5.4%, respectively. The improvement of FC and VM contents directly elevated the fuel ratio of the Co-HTC products. The highest heating value of co-hydrochar (23.4 MJ/kg) was slightly higher than individual HTC

samples, indicating it may be affected by the synergistic effects of the Co-HTC process towards enhancement of the fuel property of the hydrochar sample. However, during the Co-HTC process, organic and inorganic elements are converted into water-soluble byproducts performing the solvents in the HTC system, such as HCl, H<sub>2</sub>SO<sub>4</sub>, and other organic acids [44]. This phenomenon improves the alkali and alkali earth metal solubility contained in raw biomass feedstock, and it directly results in the enhancement of the ash removal efficiency of the hydrochar products. However, decreased inorganic elements can directly improve the calorific value of hydrochar.

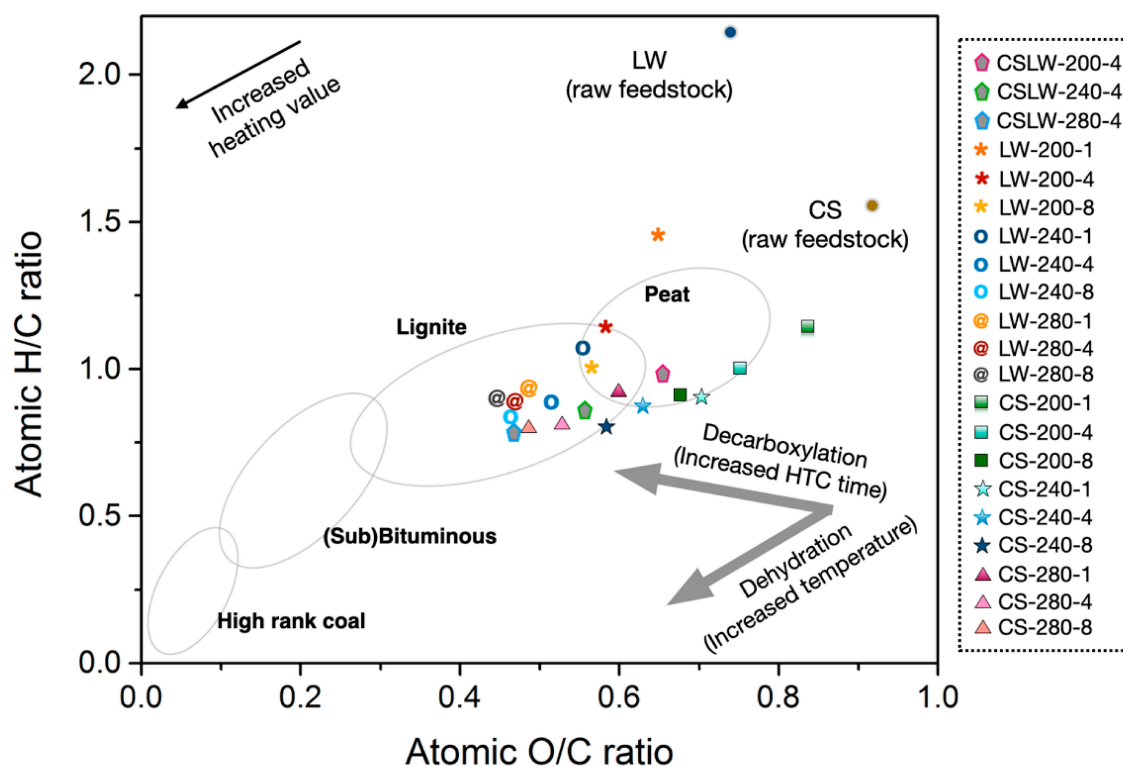


**Figure 2.** Van Krevelen's diagram of the raw feedstocks and the hydrochar products.

The fuel quality of raw CS, LW feedstock, and hydrochar products compared with natural coal is displayed in Van Krevelen's diagram, as seen in Figure 2. The pathways of decarboxylation and decarbonylation can evaluate the atomic O/C and H/C ratio depicted in Van Krevelen's diagram during the HT process, which indicates the degree of carbonization [45]. According to the diagram, the result shows that the raw CS and raw LW similarly have poor fuel quality due to their highly oxygenated compounds. This finding was supported by proximate and ultimate analyses, also listed in Table 1. However, hydrochar and co-hydrochar products produced better fuel quality than raw feedstock. The results indicated that the HTC and Co-HTC processes improved the fuel characteristics.

Moreover, increasing temperature and reaction time significantly improved the fuel quality of hydrochar and co-hydrochar due to side hydrothermal reactions, such as dehydration, decarboxylation, decarbonylation, and aromatization [46]. However, the blend feedstock obtained from the Co-HTC process shows a fuel quality in line with conventional HTC products. On the other hand, the blend feedstocks and increasing reaction temperature substantially supported removing elemental nitrogen content, as evident in Table 1. The hydrochar samples obtained at 240 and 280 °C show the atomic O/C and H/C ratios located in the area of lignite coal, as illustrated in Van Krevelen's diagram. Finding results imply that HTC and Co-HTC processes successfully achieve organic waste conversion into alternative solid fuel. Noticeably, the reaction temperature and time of HTC and Co-HTC processes are significant factors for fuel quality improvement. The increase in temperature during the hydrothermal process reached the vaporization of the water medium, which essentially promoted the thermal decomposition of raw feedstock [47].

**Table 3.** Sulfur and chlorine content of the hydrochars and co-hydrochar.

Samples	Conditions		S (%)	Cl (%)
	T (°C)	t (h)		
Corn stalk (CS)	200	1	0.16	0.3
		4	0.11	n.d.
		8	0.06	n.d.
	240	1	0.12	0.2
		4	0.04	n.d.
		8	n.d.	n.d.
	280	1	0.07	0.3
		4	0.09	0.1
		8	0.05	n.d.
Leather waste (LW)	200	1	0.12	0.6
		4	0.07	0.2
		8	n.d.	n.d.
	240	1	0.05	0.4
		4	n.d.	n.d.
		8	n.d.	n.d.
	280	1	0.03	0.4
		4	0.03	0.2
		8	n.d.	0.2
CSLW (blended feedstock)	200		0.09	0.3
	240	4	n.d.	n.d.
	280		n.d.	n.d.

Table 3 evaluated the leaching performance of sulfur and chlorine during HTC and Co-HTC processes with different hydrothermal treatment conditions. Also, the synergistic effects of blended feedstock for the Co-HTC for ash removal were studied. The initial sulfur and chlorine contents of feedstocks significantly decreased after the hydrothermal process,

compared to Table 1. The organic S and Cl were chemically released into the liquid fraction during HTC and Co-HTC processes, increasing ash leaching efficiency. In general, the organic S and Cl have very high-water solubility. Therefore, the existing leaching process during hydrothermal treatment efficiently removes high water-solubility elemental composition [41,44]. The S and Cl contents significantly decreased with increased HTC and Co-HTC temperature and extension operating time. These results correlated with the previous study [44]. For the Co-HTC process, the co-hydrochar obtained at 240 °C contains no S and Cl contents. Traditionally, air pollutants, such as  $\text{SO}_x$ ,  $\text{NO}_x$ , and Cl gas, are directly released from solid fuel combustion. Therefore, reducing air emissions can be controlled by upgrading fuel quality. However, the total ash content of hydrochar and co-hydrochar products obtained from different hydrothermal treatment conditions significantly decreased due to the elemental leaching phenomena during HTC and Co-HTC processes [46,47]. The hydrochar samples containing lower ash content may have a higher heating value than hydrochars containing high ash content, as demonstrated in Table 2. Figure 3 shows HTC and Co-HTC performances toward hydrochar production yield (HY), energy yield (EY), and enhancement ratio. The Co-HTC process was barely studied by using a Co-HTC period of 4 h due to minimizing the total ash of hydrochar products. Figures 3a and b show that the increase in temperature from 200 °C to 280 °C led to a significant decrease in the mass yield of hydrothermal-treated CS and LW that corresponded to the hydrothermal decomposition of chemical structures for corn stalk and leather waste [47,48]. The mass yield continually decreased at 52.5% and 36.9% for CS and LW samples obtained at 280 °C for 4 h, respectively. The mass yield of produced hydrochar significantly increased at the HTC condition of 280 °C 8 h, indicating the re-polymerization coincided with the HTC process at the high-temperature condition [48]. The production yields of co-hydrochar were in a similar trend as the production yield of conventional hydrochar (Figure 3c). However, co-hydrochar products exhibited a higher mass yield. The production yields of co-hydrochar were approximately between 53.8%–74.6%, indicating that the effect of the Co-HTC process ascribed to the deposition of leather waste on the cornstalk substrate [30,49]. The main reason for the lower mass yield is the higher hydrothermal temperature, resulting in the degradation of biomass polymers.

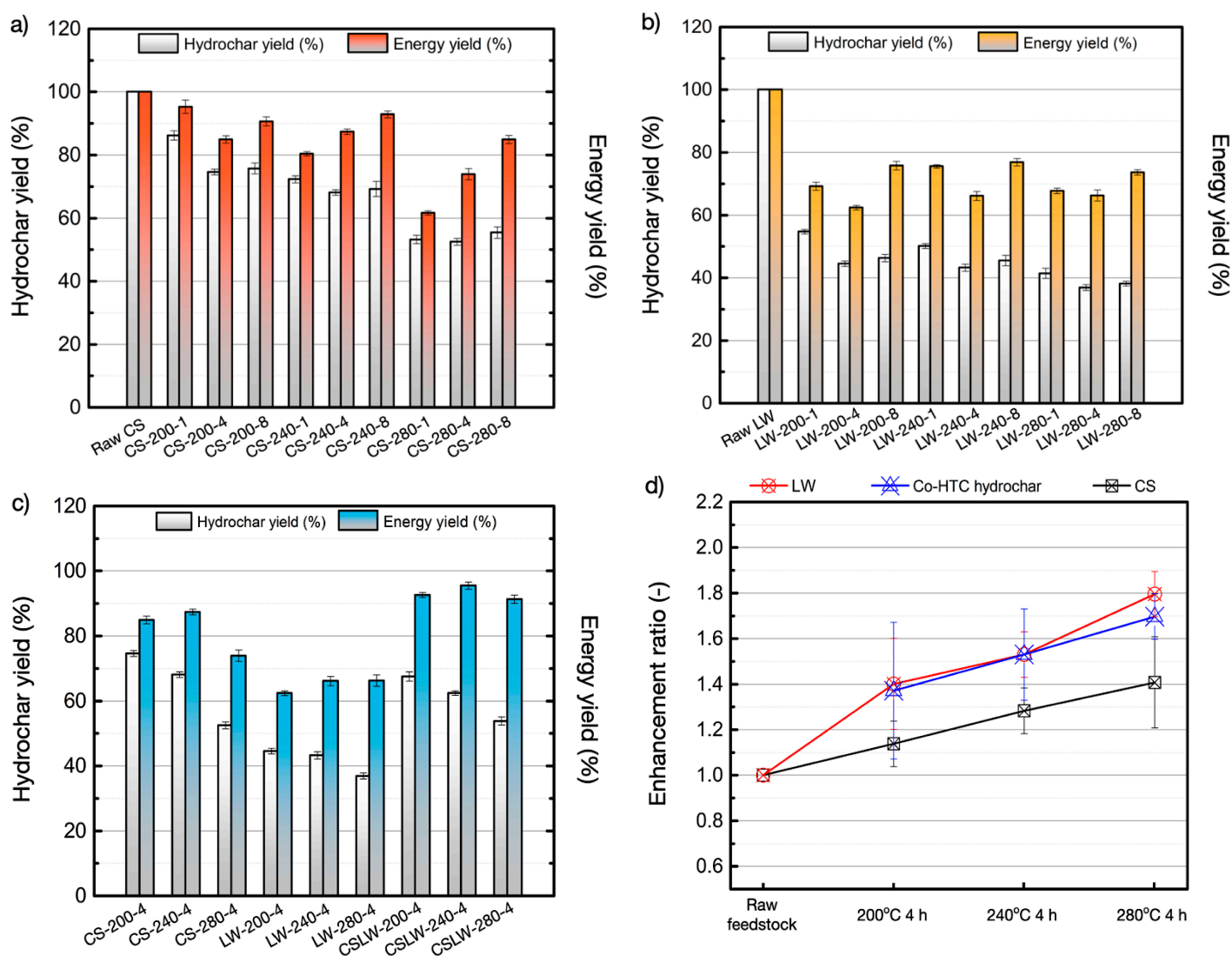


**Figure 3.** Hydrochar production yield and energy yield of (a) CS samples, (b) LW samples, (c) Blend samples at HTC reaction time of 4 h, and (d) Enhancement ratio of hydrochars and co-hydrochars.

With increased process temperature, the energy yield of CS hydrochar gradually decreased from 95.27% to 61.6%, which was in a similar trend of mass yield (Figure 3a). However, the extension of reaction time during the HTC process firstly decreased the energy yield of CS hydrochar at 1 h and then increased by raising the HTC holding time to 4 h and 8 h, respectively. Meanwhile, LW hydrochars first present the lower energy yield, then increase with increasing HTC temperature and extension of holding time, as seen in Figure 3b. These results align with the report of Ning et al. (2022) [29]. The energy yield of CS hydrochar and LW hydrochar ranged between 61.6%–95.29% and 62.36%–76.86%, respectively. As the constant holding time of 4 h, the higher energy yield was obtained from blended hydrochars in the range between 91.29%–95.49% compared to conventional hydrochars (Figure 3c). It can imply that the Co-HTC

improves hydrochar quality, which is in line with the study of Weihrich et al. (2022) [25] and Shakiba et al. (2023) [50].

In addition, Figure 3d shows the enhancement ratio (ER) of hydrochars produced at different conditions. Generally, the ER was used to explain the development of HHV of raw biomass. According to previous literature, Kuo et al. (2019) [51] and Yueh-Heng Li et al. (2020) [52] reported that an increase in reaction temperature during the biomass pretreatment process is a significant parameter for the improvement of the heating value of the resulting product. The ER value of hydrochar samples was the highest in the range of 1.41–1.81 at a hydrothermal treatment condition of 280 °C. Noticeably, the hydrothermal decomposition of oxygenated compounds in the raw biomass during high-severity conditions significantly increased the ER ratio despite the gradual decrease in mass yield and energy yield. The optimization of energy yield may become the excellent pathway for high-performance producing hydrochar by the hydrothermal treatment process.

Figure 4 displayed the SEM images of different samples, including CS and LW feedstocks, hydrochar, and Co-HTC products obtained at 280 °C for 4 h, observed by using FE-SEM at 1000× magnification. The CS and LW hydrochars showed the characteristics of dense and smooth surfaces (Figures 4a and b). After the hydrothermal treatment, the structure of CS hydrochar has various tiny pore structures visible on its surface, as seen in Figure 4c. The surface morphology of CS hydrochar in this study was also related to the SEM images reported in the previous study [53]. The degradation of biomass polymer formed the porous structure through the dehydration reaction during the HTC process. The HTC process did not break the surface morphology of LW hydrochar (Figure 4d). In addition, Figure 4e displays the SEM image of the co-hydrochar product (CSLW-280-4). The observation also verifies the combination surface appearance between CS and LW hydrochars. One possible explanation is that LW formed on the CS hydrochar surface by observing the SEM image of CSLW-280-4. The co-hydrochars show fluffy and messy morphology. Production yield improvement is possessed from the Co-HTC blending feedstocks between plastic waste and plant biomass [54]. Additionally, the porous structure with high-density solid fuel may enhance the relative completed combustion process due to the easy air access to the inner structure of solid fuel during the combustion process, ascribed to combustion theory [55]. However, the HTC and Co-HTC severity still plays a significant pathway in various surface morphology of hydrochar.

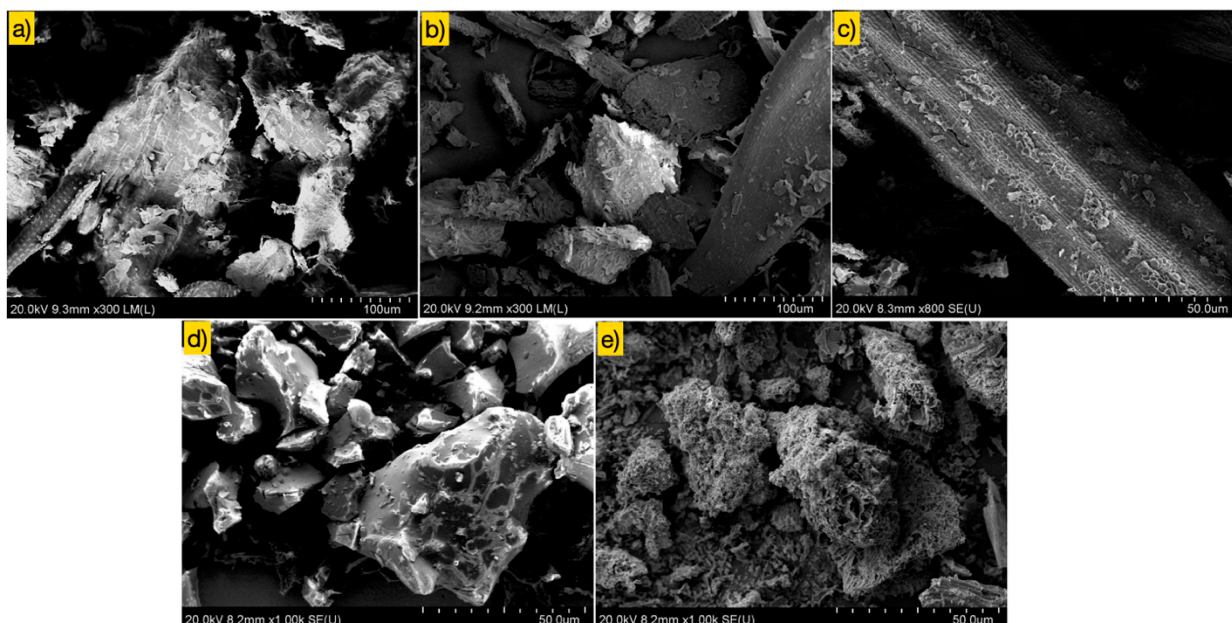


**Figure 4.** SEM micrographs of (a) Raw CS, (b) Raw LW, (c) CS-280-4, (d) LW-280-4, and (e) CSLW-280-4 (co-hydrochar).

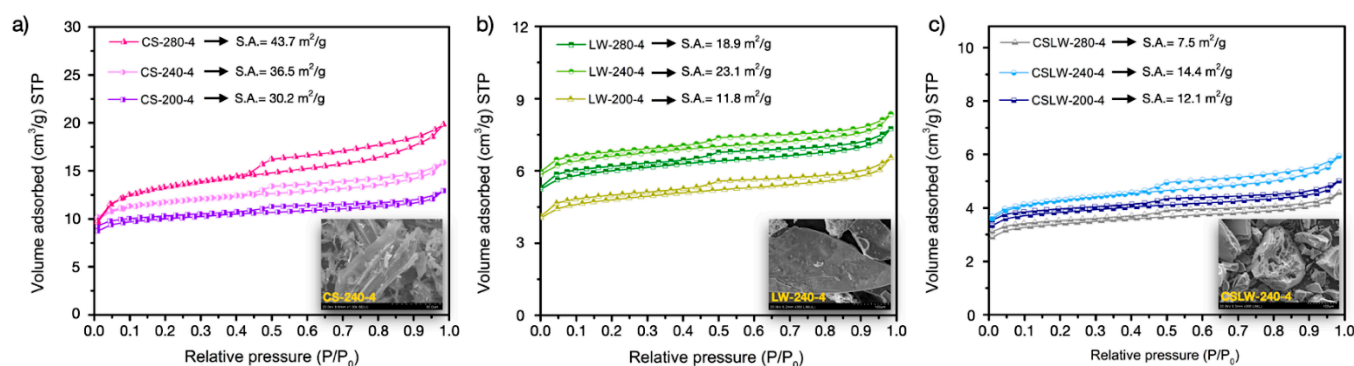


**Figure 5.** N<sub>2</sub> adsorption-desorption isotherms of hydrochar products obtained from different hydrothermal temperatures (a) CS hydrochars, (b) LW hydrochars, and (c) co-hydrochars.

Figure 5 displays N<sub>2</sub> adsorption-desorption isotherms of different resulting hydrochars, which explored the interaction of hydrochar surface between conventional hydrochars (CS and LW hydrochars), as seen in Figures 5a and b, respectively, and co-hydrochars (Figure 5c). The N<sub>2</sub> sorption isotherms exhibit Type II isotherms with a small hysteresis loop, suggesting a wide range of pore sizes, including mesopores and macropores with less porous structures [56]. The specific surface area of CS hydrochars, LW hydrochars, and co-hydrochars (CSLWs) ranged from 30.2–43.7 m<sup>2</sup>/g, 11.8–23.1 m<sup>2</sup>/g, and 7.5–14.4 m<sup>2</sup>/g, respectively. The results of the N<sub>2</sub> sorption analysis conform with the surface morphology observed by the SEM technique. The CS hydrochars typically obtain the more significant porosity with the highest surface area, while LW hydrochars and co-hydrochars have a characteristic of less porosity. This result is assured by SEM micrographs, as demonstrated in Figure 4. However, the

LW aggregated to CS hydrochars during the Co-HTC process also seemingly contributes to increasing hydrochar production yield and energy yield for the co-hydrochar samples (seen in SEM micrographs). Regarding  $N_2$  adsorption analysis, it can imply that  $N_2$  sorption isotherms can efficiently explain the synergistic effects of the Co-HTC process by the metamorphosis of hydrochar surface characteristics, which could affect other fuel properties.

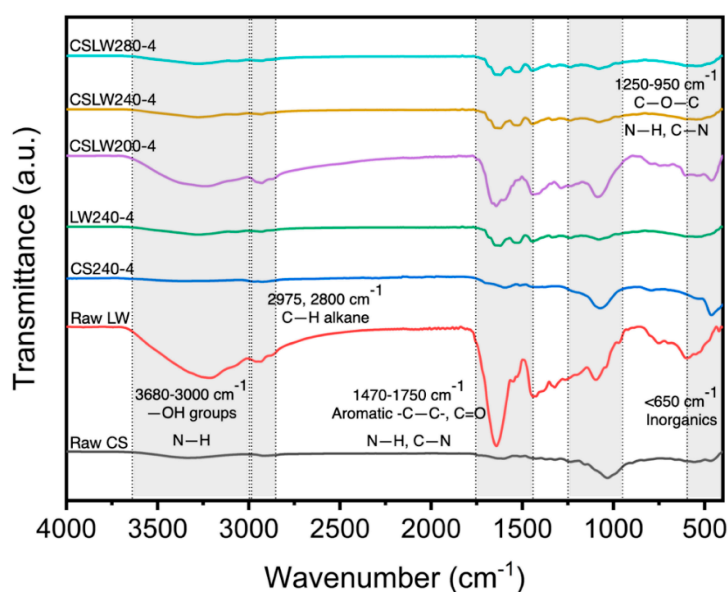


**Figure 6.** FTIR spectra of CS feedstock, LW feedstock, conventional hydrochars, and co-hydrochars.

Figure 6 displays the Fourier transform infrared spectroscopy (FTIR) spectra, which evaluates the characteristics of surface functional groups for different samples, including raw CS feedstock, raw LW feedstock, hydrochars produced at 240 °C for 4 h, and co-hydrochars produced at different HTC temperatures of 200, 240, and 280 for 4 h. The FTIR spectra were observed in the wavelength between 4000–400  $cm^{-1}$  using transmittance mode. For CS surface functional groups obtained from the FTIR technique, the small broad peak between 3680–3000  $cm^{-1}$  ascribes the vibration of –OH stretching of hydroxyl and carbonyl groups contained in lignin, which is commonly a chemical component of plant-based biomass. Also, the bands located at 1600 and 1512  $cm^{-1}$  were ascribed to –C–C– of lignin [57]. The vibration peaks center at 2975 and 2800  $cm^{-1}$  are associated with the C–H stretching of aliphatic compounds for polysaccharides in the hemicellulose and cellulose [58], While the broad peak between 1470–1750  $cm^{-1}$  ascribed to the C=O stretching in carbonyl and ester groups of hemicellulose, cellulose and lignin components. The vibration bands located at 1250–950  $cm^{-1}$  mainly correspond to the C–O–C vibration of hemicellulose and cellulose content [43]. In addition, LW feedstock shows the different characteristics of the FTIR spectrum due to

animal waste-derived biomass. In the FTIR spectrum, a significant vibration was observed around the band centered at  $3300\text{ cm}^{-1}$ , mainly ascribed to N–H stretching. Moreover, the high-intensity peak located at  $1660\text{ cm}^{-1}$  correlated with C=O stretching in amides, which substantially decreased by hydrothermal treatment. The intensity of the broadband around  $1470\text{--}1560\text{ cm}^{-1}$  shows a combination signal of N–H and C–N stretching vibrations in the collagen amide groups [59].

In addition, the intense peak at around  $1240\text{ cm}^{-1}$  corresponds to the N–H and C–N blending vibration related to amide groups and the  $\text{CH}_2$  bonding vibration in a structure of protein and glycine linkages [60]. Previous studies implied that the characteristic of ash constituents contained in biomass structure was at the intensity band below  $650\text{ cm}^{-1}$  [61,62]. However, the surface functional groups of hydrochar and co-hydrochar products were noticeably decomposed and correlated with the severity of the hydrothermal condition. The enhancement of the carbonization degree during the hydrothermal treatment process is variable by raising the temperature, which is directly beneficial for the endothermic reaction. Process temperature and time increases significantly decompose the oxygenated functional groups by dehydration, DCO, and  $\text{DCO}_2$  reactions, which became less intense FTIR spectra. This phenomenon directly reduced O, H contents (See ultimate analysis in Table 2). However, the FTIR spectra of LW hydrochar and co-hydrochar samples show the reduction of N-functional groups. This result indicates that the denitrification reaction occurred simultaneously during the HTC and Co-HTC processes, gradually decreasing the N percentage [63]. This finding is also evident by ultimate analyses. The weak intensity band correlated to oxygenated groups on FTIR spectra of hydrochar and co-hydrochar products reveals the purity of carbon content achieved from the hydrothermal treatment. This result also corresponds to the aromatic carbon structure (C=C) at the band between  $1530\text{--}1500\text{ cm}^{-1}$ , shown in FTIR spectra of all resulting hydrochar products.

### **Hygroscopic Properties of Hydrochar and Co-Hydrochar Products**

In theory, measuring the contact angle of water droplets and equilibrium moisture content (EMC) is widely explored for the hydrophobicity of biomass and biomass-derived solid fuel. Moreover, biomass hygroscopicity reduction extent (HRE) represents the reduction of biomass hygroscopicity. Figure 7 displays the EMC and HRE profiles with a relationship of % mass loss for different feedstocks and hydrochar samples. The EMC values of different hydrochars substantially declined, following the mass loss trend, which occurred with increasing hydrothermal severity. The findings could be explained by the

dehydration of oxygen compounds through the thermal decomposition during HTC and Co-HTC processes (see Figure 7a). It is also evident in the report from a previous study [64]. The co-hydrochar exhibited a higher EMC value due to its synergistic effect on the carbon atom deposition between leather waste and corn stalk during the Co-HTC process. However, the lower ash content of co-hydrochar may improve their HRE because more ash composition presents more hydrophilicity [65]. This result also correlates with the proximate analyses listed in Table 2. In addition, the hydrophobicity of hydrochar samples is in line with the increase in HRE values (Figure 7b). The highest HRE also presents for co-hydrochar, reaching up to 70.14% at a Co-HTC condition of 280 °C for 4 h. The thermal conversion process could achieve the development of EMC. Wei-Hsin Chen et al. (2018) reported that the HRE profile of fir residues was enhanced entirely as high as 57.39% by the conventional torrefaction at 230 °C [66].

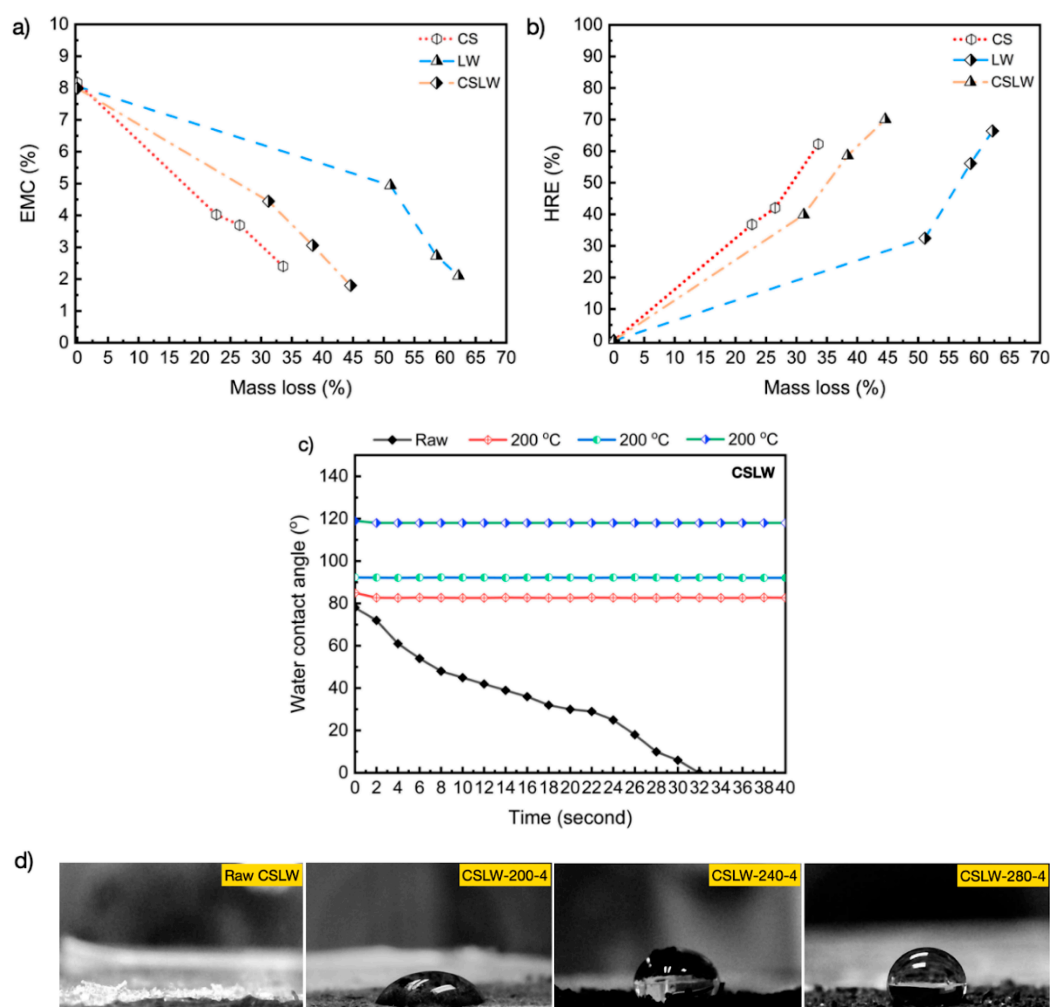


**Figure 7.** Hygroscopic properties of raw feedstocks and hydrochar products (a) Equilibrium moisture content; EMC, (b) Hygroscopicity reduction extent; HRE, (c) Profile of water contact angle, and (d) Appearance of contact angle on co-hydrochar surface.

Nonetheless, Figure 7c shows profiles of contact angles operated using a high-resolution optical camera with a video measurement system between 0–40 s. The hydrophilic surface of biomass presents the water contact angle near 0°. Figure 7d shows the appearance of the hydrophilic surface of blended feedstock (CSLW). The initial water contact angle of 79.3° on the surface of raw CSLW becomes 0° approximately in 32 s, showing that raw biomass essentially has a hygroscopic nature. Meanwhile, the HTC and Co-HTC processes caused the increasing water contact angle, resulting in more hydrophobicity. The constant water contact angle found on the surface of co-hydrochars produced at 240 and 280 °C, respectively. The contact angle of hydrochar produced at harsh conditions (280 °C, contact angle of 119.5°) is specifically higher than in mild conditions (200 °C, contact angle of 82.7°, and 240 °C, contact angle 104.3°). It can imply that co-hydrochar produced at 280 °C exhibited a superior hydrophobic property. The hydrophilic property of raw biomass is mainly because of existing oxygenated functional groups in their chemical structure, including hydroxyl (–OH), carbonyl (C=O), and carboxylic acid groups (COOH) for plant-based biomass [58,67], while amide (N–H) and nitrile (C–N) groups for leather waste contain a protein structure [59]. Hence, eliminating the mentioned functional groups through the hydrothermal treatment process improves hydrophobicity. Improving hygroscopic behavior after the hydrothermal treatment can improve solid fuel stability and biodegradation properties [62,66].

## CONCLUSIONS

This current study demonstrates the potential of hydrothermal carbonization (HTC) and co-hydrothermal carbonization (Co-HTC) processes in producing a sustainable solid biofuel from corn stalk residue and leather waste that examined the effects of HTC and Co-HTC at reaction temperatures of 200, 240, and 280 °C and hydrothermal treatment durations of 1, 4, and 8 h. Finding results showed that the severity of HTC and Co-HTC substantially caused the improvement of physicochemical properties and fuel characteristics of hydrochar products due to the release of some volatile matters and the loss of ash content. Moreover, the corrosive elements, including sulfur, chlorine, and nitrogen, were accomplished removed after the HTC and Co-HTC processes. Also, the leaching of total ash content of hydrochar was significantly reduced up to 44.52% for the condition of residence time of 4 h.

Moreover, a long period of residence time significantly promoted the reconstruction of ash due to the re-polymerization of the hydrothermal treatment process. The Co-HTC exhibited a synergistic effect towards achieving superior fuel quality, such as higher energy yield and lower total ash content. However, hydrochar and co-hydrochar products have a heating value of 16.8–23.4 MJ/kg after hydrothermal processing. The

resulting hydrochar has the potential as a bio-solid fuel substitute for solid fossil fuels for heat production. The hygroscopicity reduction extend (HRE) measured the hygroscopic nature of samples. The hydrochar products have an HRE value in the range of 31.38%–70.14%, indicating the transformation of the hydrophilic nature of biomass into hydrophobic behavior resulted in high resistance to microbial degradation and prolonging the storage period of hydrochar products. Overall, the finding results from this study showed that HTC and Co-HTC are effective thermochemical conversion processes for improving the fuel quality of biomass feedstock. Moreover, it could fulfill designing experiments in a pilot-scale HTC and Co-HTC processes of corn stalk residue, leather waste, and their blended feedstock.

#### **DATA AVAILABILITY**

All data generated or analyzed during this study are included in this published article.

#### **AUTHOR CONTRIBUTIONS**

NK and AE: Conceptualization, Methodology; NK and SC: Experiment and Investigation; NK and SC: Writing-original draft preparation, and Revision; SC: Software; KM and AE: Funding acquisition, conceptualization, project administration, and supervision, writing review and editing. All authors read and approved the final manuscript.

#### **CONFLICTS OF INTEREST**

All authors declare no conflicts of interest.

#### **FUNDING**

The Kasetsart University Research and Development Institute (KURDI, grant number: YF(KU)4.65) acknowledges the financial support.

#### **ACKNOWLEDGMENTS**

The authors acknowledge the College of Material Innovation and Technology, King Mongkut's Institute of Technology Ladkrabang, and the Department of Mechanical Engineering, Faculty of Engineering, Kasetsart University Kampaeng Saen Campus, for supporting this research.

#### **REFERENCES**

1. Hussain N, Ahmed M, Duangpan S, Hussain T, Taweekun J. Potential Impacts of Water Stress on Rice Biomass Composition and Feedstock Availability for Bioenergy Production. *Sustainability*. 2021;13(18):10449.
2. Schmitt N, Apfelbacher A, Jäger N, Daschner R, Stenzel F, Hornung A. Thermochemical conversion of biomass and upgrading to biofuel: The Thermo-

- Catalytic Reforming process—A review. *Biofuel Bioprod Biorefin.* 2019;13(3):822-37.
3. Wang W, Porninta K, Aggarangsi P, Leksawasdi N, Li L, Chen X, et al. Bioenergy development in Thailand based on the potential estimation from crop residues and livestock manures. *Biomass Bioenergy.* 2021;144:105914.
  4. Huang CW, Hsieh CH, Lasek J, Li YH. Optimal Fe/Ni/Ca-Al catalyst for tar model steam reforming by using the Taguchi method. *Int J Energy Res.* 2022;46(6):7799-815.
  5. Chaichaloempreecha A, Chunark P, Hanaoka T, Limmeechokchai B. Thailand's mid-century greenhouse gas emission pathways to achieve the 2 degrees Celsius target. *Energy Sustain Soc.* 2022;12(1):1-20.
  6. Yang B, Wei YM, Liu LC, Hou YB, Zhang K, Yang L, et al. Life cycle cost assessment of biomass co-firing power plants with CO<sub>2</sub> capture and storage considering multiple incentives. *Energy Econ.* 2021;96:105173.
  7. Deng L, Zhang T, Che D. Effect of water washing on fuel properties, pyrolysis and combustion characteristics, and ash fusibility of biomass. *Fuel Process Technol.* 2013;106:712-20.
  8. Fu J, Wang J. Enhanced slurryability and rheological behaviors of two low-rank coals by thermal and hydrothermal pretreatments. *Powder Technol.* 2014;266:183-90.
  9. Ge L, Feng H, Xu C, Zhang Y, Wang Z. Effect of hydrothermal dewatering on the pyrolysis characteristics of Chinese low-rank coals. *Appl Therm Eng.* 2018;141:70-8.
  10. Huang C, Wu X, Huang Y, Lai C, Li X, Yong Q. Prewashing enhances the liquid hot water pretreatment efficiency of waste wheat straw with high free ash content. *Bioresour Technol.* 2016;219:583-8.
  11. Kwan WH, Wong YS. Acid leached rice husk ash (ARHA) in concrete: A review. *Mat Sci Energy Technol.* 2020;3:501-7.
  12. Mahedi M, Cetin B, Dayioglu AY. Effect of cement incorporation on the leaching characteristics of elements from fly ash and slag treated soils. *J Environ Manage.* 2020;253:109720.
  13. Loginova E, Proskurnin M, Brouwers HJH. Municipal solid waste incineration (MSWI) fly ash composition analysis: A case study of combined chelant-based washing treatment efficiency. *J Environ Manage.* 2019;235:480-8.
  14. Reza MT, Emerson R, Uddin MH, Gresham G, Coronella CJ. Ash reduction of corn stover by mild hydrothermal preprocessing. *Biomass Conv Bioref.* 2015;5:21-31.
  15. Wang L, Tang Y, Gong Y, Shao X, Lin X, Xu W, et al. Remediation of Micro-Pollution in an Alkaline Washing Solution of Fly Ash Using Simulated Exhaust Gas: Parameters and Mechanism. *Sustainability.* 2023;15(7):5873.
  16. Yoo HM, Park SW, Jeong YO, Han GH, Choi HS, Seo YH. Enhancement of Gasification Performance for Palm Oil Byproduct by Removal of Alkali and Alkaline Earth Metallic Compounds and Ash. *Energy Fuels.* 2019;33(6):5263-9.
  17. de Jager M, Röhrdanz M, Giani L. The influence of hydrochar from biogas digestate on soil improvement and plant growth aspects. *Biochar.* 2020;2(2):177-94.

18. Enaime G, Baçaoui A, Yaacoubi A, Wichern M, Lübken M. Hydrothermal carbonization of the filter bed remained after filtration of olive mill wastewater on olive stones for biofuel application. *Biomass Conv Bioref.* 2020;12(4):1237-47.
19. Tsarpali M, Arora N, Kuhn JN, Philippidis GP. Beneficial use of the aqueous phase generated during hydrothermal carbonization of algae as nutrient source for algae cultivation. *Algal Res.* 2021;60:102485.
20. Hossain N, Nizamuddin S, Griffin G, Selvakannan P, Mubarak NM, Mahlia TMI. Synthesis and characterization of rice husk biochar via hydrothermal carbonization for wastewater treatment and biofuel production. *Sci Rep.* 2020;10(1):18851.
21. Kang K, Nanda S, Sun G, Qiu L, Gu Y, Zhang T, et al. Microwave-assisted hydrothermal carbonization of corn stalk for solid biofuel production: Optimization of process parameters and characterization of hydrochar. *Energy.* 2019;186:115795.
22. Lee J, Hong J, Jang D, Park KY. Hydrothermal carbonization of waste from leather processing and feasibility of produced hydrochar as an alternative solid fuel. *J Environ Manage.* 2019;247:115-20.
23. Pauline AL, Joseph K. Hydrothermal carbonization of oily sludge for solid fuel recovery—investigation of chemical characteristics and combustion behaviour. *J Anal Appl Pyrolysis.* 2021;157:105235.
24. Mariuzza D, Lin JC, Volpe M, Fiori L, Ceylan S, Goldfarb JL. Impact of Co-Hydrothermal carbonization of animal and agricultural waste on hydrochars' soil amendment and solid fuel properties. *Biomass Bioenergy.* 2022;157:106329.
25. Weihrich S, Xing X, Zhang X. Co-pyrolysis and HTC refined biomass-biosolid-mixes: combustion performance and residues. *Int J Energy Environ Eng.* 2022;13(2):657-69.
26. Zhang X, Zhang L, Li A. Co-hydrothermal carbonization of lignocellulosic biomass and waste polyvinyl chloride for high-quality solid fuel production: Hydrochar properties and its combustion and pyrolysis behaviors. *Bioresour Technol.* 2019;294:122113.
27. Saba A, Saha P, Reza MT. Co-Hydrothermal Carbonization of coal-biomass blend: Influence of temperature on solid fuel properties. *Fuel Process Technol.* 2017;167:711-20.
28. Kahilu GM, Bada S, Mulopo J. Physicochemical, structural analysis of coal discards (and sewage sludge) (co)-HTC derived biochar for a sustainable carbon economy and evaluation of the liquid by-product. *Sci Rep.* 2022;12(1):17532.
29. Ning X, Dang H, Xu R, Wang G, Zhang J, Zhang N, et al. Co-hydrothermal carbonization of biomass and PVC for clean blast furnace injection fuel production: Experiment and DFT calculation. *Renew Energy.* 2022;187:156-68.
30. Poomsawat S, Poomsawat W. Effect of co-hydrothermal carbonization of sugarcane bagasse and polyvinyl chloride on co-production of furfural and solid fuel. *Bioresour Technol Rep.* 2022;19:101206.

31. Xu Z, Qi R, Zhang D, Gao Y, Xiong M, Chen W. Co-hydrothermal carbonization of cotton textile waste and polyvinyl chloride waste for the production of solid fuel: Interaction mechanisms and combustion behaviors. *J Clean Prod.* 2021;316:128306.
32. de Jager M, Schröter F, Wark M, Giani L. The stability of carbon from a maize-derived hydrochar as a function of fractionation and hydrothermal carbonization temperature in a Podzol. *Biochar.* 2022;4(1):52.
33. Lee J, Lee K, Sohn D, Kim YK, Park KY. Hydrothermal carbonization of lipid extracted algae for hydrochar production and feasibility of using hydrochar as a solid fuel. *Energy.* 2018;153:913-20.
34. Zhang S, Su Y, Xu D, Zhu S, Zhang H, Liu X. Assessment of hydrothermal carbonization and coupling washing with torrefaction of bamboo sawdust for biofuels production. *Bioresour Technol.* 2018;258:111-8.
35. Krysanova K, Krylova A, Zaichenko V, Lavrenov V, Khaskhachikh V. Influence of the parameters of the hydrothermal carbonization of the biomass on the biocoal obtained from peat. *E3S Web Conf.* 2019;114:07003.
36. Song Y, Zhan H, Zhuang X, Yin X, Wu C. Synergistic Characteristics and Capabilities of Co-hydrothermal Carbonization of Sewage Sludge/Lignite Mixtures. *Energy Fuels.* 2019;33(9):8735-45.
37. Mazumder S, Saha P, Reza MT. Co-hydrothermal carbonization of coal waste and food waste: fuel characteristics. *Biomass Conv Bioref.* 2020;12(1):3-13.
38. Ferreira SD, Altafini CR, Perondi D, Godinho M. Pyrolysis of Medium Density Fiberboard (MDF) wastes in a screw reactor. *Energy Convers Manag.* 2015;92:223-33.
39. Aston JE, Wahlen BD, Davis RW, Siccardi AJ, Wendt LM. Application of aqueous alkaline extraction to remove ash from algae harvested from an algal turf scrubber. *Algal Res.* 2018;35:370-7.
40. Liu H, Chen Y, Yang H, Gentili FG, Söderlind U, Wang X, et al. Hydrothermal carbonization of natural microalgae containing a high ash content. *Fuel.* 2019;249:441-8.
41. Wang W, Wen C, Chen L, Liu T, Li C, Liu E, et al. Effect of combining water washing and carbonisation on the emissions of PM10 generated by the combustion of typical herbs. *Fuel Process Technol.* 2020;200:106311.
42. Guan Y, Liu C, Peng Q, Zaman F, Zhang H, Jin Z, et al. Pyrolysis kinetics behavior of solid leather wastes. *Waste Manag.* 2019;100:122-7.
43. Kanchanatip E, Prasertsung N, Thasnas N, Gridanurak N, Wantala K. Valorization of cannabis waste via hydrothermal carbonization: solid fuel production and characterization. *Environ Sci Pollut Res Int.* 2023;30:90318-27.
44. Wang T, Zhai Y, Zhu Y, Gan X, Zheng L, Peng C, et al. Evaluation of the clean characteristics and combustion behavior of hydrochar derived from food waste towards solid biofuel production. *Bioresour Technol.* 2018;266:275-83.
45. Libra JA, Ro KS, Kammann C, Funke A, Berge ND, Neubauer Y, et al. Hydrothermal carbonization of biomass residuals: a comparative review of the chemistry, processes and applications of wet and dry pyrolysis. *Biofuels.* 2014;2(1):71-106.

46. Khan MA, Hameed BH, Siddiqui MR, Alothman ZA, Alsohaimi IH. Physicochemical, structural and combustion analyses to estimate the solid fuel efficacy of hydrochar developed by co-hydrothermal carbonization of food and municipal wastes. *Biomass Conv Bioref.* 2022. doi: 10.1007/s13399-022-02875-6
47. Zhao J, Liu C, Hou T, Lei Z, Yuan T, Shimizu K, et al. Conversion of biomass waste to solid fuel via hydrothermal co-carbonization of distillers grains and sewage sludge. *Bioresour Technol.* 2022;345:126545.
48. Qi R, Xu Z, Zhou Y, Zhang D, Sun Z, Chen W, et al. Clean solid fuel produced from cotton textiles waste through hydrothermal carbonization with FeCl<sub>3</sub>: Upgrading the fuel quality and combustion characteristics. *Energy.* 2021;214:118926.
49. Fakudze S, Wei Y, Shang Q, Ma R, Li YH, Chen J, et al. Single-pot upgrading of run-of-mine coal and rice straw via Taguchi-optimized hydrothermal treatment: Fuel properties and synergistic effects. *Energy.* 2021;236:121482.
50. Shakiba A, Aliasghar A, Moazeni K, Pazoki M. Hydrothermal Carbonization of Sewage Sludge with Sawdust and Corn Stalk: Optimization of Process Parameters and Characterization of Hydrochar. *Bioenerg Res.* 2023. doi: 10.1007/s12155-022-10552-9
51. Kuo WC, Lasek J, Słowik K, Głód K, Jagustyn B, Li YH, et al. Low-temperature pre-treatment of municipal solid waste for efficient application in combustion systems. *Energy Convers Manag.* 2019;196:525-35.
52. Li YH, Kuo WC. The study of optimal parameters of oxygen-enriched combustion in fluidized bed with optimal torrefied woody waste. *Int J Energy Res.* 2020;44(9):7416-34.
53. Ge Z, Cao X, Zha Z, Ma Y, Zeng M, Wu Y, et al. The influence of a two-step leaching pretreatment on the steam gasification properties of cornstalk waste. *Bioresour Technol.* 2022;358:127403.
54. Yu Y, Zhu B, Ding Y, Li P, Ge S. Hydrothermal carbonization of food waste digestates and polyvinyl chloride: focus on dechlorination performance and fuel characteristics. *Biomass Conv Bioref.* 2022. doi: 10.1007/s13399-022-02957-5
55. Chen R, Sheng Q, Dai X, Dong B. Upgrading of sewage sludge by low temperature pyrolysis: Biochar fuel properties and combustion behavior. *Fuel.* 2021;300:121007.
56. Gao QL, Li DS, Liu XM, Wang YF, Liu WL, Ren MM, et al. Biomass-derived mesoporous carbons materials coated by  $\alpha$ -Mn<sub>3</sub>O<sub>4</sub> with ultrafast zinc-ion diffusion ability as cathode for aqueous zinc ion batteries. *Electrochim Acta.* 2020;335:135642.
57. Kaewtrakulchai N, Faungnawakij K, Eiad-Ua A. Parametric Study on Microwave-Assisted Pyrolysis Combined KOH Activation of Oil Palm Male Flowers Derived Nanoporous Carbons. *Materials.* 2020;13(12):2876.
58. Manatura K, Chalermssinsuwan B, Kaewtrakulchai N, Chao YH, Li YH. Co-torrefaction of rice straw and waste medium density fiberboard: A process optimization study using response surface methodology. *Results Eng.* 2023;18:101139.

59. Lakraflı H, Tahiri S, Albizane A, Bouhria M, El Otmani ME. Experimental study of thermal conductivity of leather and carpentry wastes. *Constr Build Mater.* 2013;48:566-74.
60. Kong J, Yue Q, Wang B, Huang L, Gao B, Wang Y, et al. Preparation and characterization of activated carbon from leather waste microwave-induced pyrophosphoric acid activation. *J Anal Appl Pyrolysis.* 2013;104:710-3.
61. Bandara YW, Gamage P, Gunarathne DS. Hot water washing of rice husk for ash removal: The effect of washing temperature, washing time and particle size. *Renew Energy.* 2020;153:646-52.
62. Chen D, Zheng Z, Fu K, Zeng Z, Wang J, Lu M. Torrefaction of biomass stalk and its effect on the yield and quality of pyrolysis products. *Fuel.* 2015;159:27-32.
63. Islam MT, Reza MT. Evaluation of fuel and combustion properties of hydrochar derived from Co-hydrothermal carbonization of biomass and plastic. *Biomass Bioenergy.* 2023;172:106750.
64. Mei Y, Liu R, Yang Q, Yang H, Shao J, Draper C, et al. Torrefaction of cedarwood in a pilot scale rotary kiln and the influence of industrial flue gas. *Bioresour Technol.* 2015;177:355-60.
65. Zhang C, Wang M, Chen WHH, Zhang Y, Pétrissans A, Pétrissans M, et al. Superhydrophobic and superlipophilic biochar produced from microalga torrefaction and modification for upgrading fuel properties. *Biochar.* 2023;5(1):18.
66. Chen WH, Lin BJ, Colin B, Chang JS, Pétrissans A, Bi X, et al. Hygroscopic transformation of woody biomass torrefaction for carbon storage. *Appl Energy.* 2018;231:768-76.
67. Sun Z, Dai L, Lai P, Shen F, Shen F, Zhu W. Air oxidation in surface engineering of biochar-based materials: a critical review. *Carbon Res.* 2022;1(1):32.

How to cite this article:

Kaewtrakulchai N, Chanpee S, Manatura K, Eiad-Ua A. Upgrading of Corn Stalk Residue and Tannery Waste into Sustainable Solid Biofuel via Conventional Hydrothermal Carbonization and Co-Hydrothermal Carbonization. *J Sustain Res.* 2023;5(3):e230012. <https://doi.org/10.20900/jsr20230012>